

Surface Aspects of Bismuth–Metal Oxide Catalysts

Navneet Arora,* Goutam Deo,* Israel E. Wachs,*¹ and Andrew M. Hirt†

*Zettlemoyer Center for Surface Studies, Department of Chemical Engineering, Lehigh University, Bethlehem, Pennsylvania 18015; and

†Materials Research Laboratories, Inc., 290 North Bridge Street, Struthers, Ohio 44471

Received May 9, 1994; revised October 20, 1995; accepted October 23, 1995

A series of conventional and model bismuth–metal oxide catalysts (vanadates, molybdates, tungstates, and niobates) were physically and chemically characterized (Raman spectroscopy, BET, XPS, and methanol oxidation) to obtain additional insights into the structure-reactivity relationships of such catalytic materials. The reactivity for methanol oxidation over the conventional bismuth–metal oxide catalysts was found to be primarily related to the surface area of the oxide catalysts and was essentially independent of the near surface composition and the bulk structure. The selectivity for methanol oxidation over the conventional bismuth–metal oxide catalysts was essentially found not to be a function of the surface area, the near surface composition, and the bulk structure. A series of model bismuth–metal oxide catalysts was synthesized by depositing metal oxides on the surface of a bismuth oxide support. The model studies demonstrated that two-dimensional metal oxide overlayers are not stable on the bismuth oxide support and readily react to form bulk bismuth–metal oxide compounds upon heating. Furthermore, the model studies revealed that these bulk bismuth–metal oxide compounds are related to the active sites for the partial oxidation reaction. *In situ* Raman spectroscopy in methanol/oxygen, methanol, and oxygen reaction environments with helium as the diluent revealed no additional information regarding the nature of the active site. It was found that only highly crystalline bismuth–metal oxide phases are selective for the partial oxidation of methanol to formaldehyde. Thus, selective bismuth–metal oxide catalysts will always possess highly crystalline metal oxide phases containing extremely low surface areas which make it difficult to obtain fundamental surface information about the outermost layers. © 1996

Academic Press, Inc.

INTRODUCTION

Bulk metal oxides find extensive application as catalysts for industrial selective oxidation reactions. In particular, the ternary oxides derived from bismuth oxide exhibit a variety of interesting physical and chemical properties. Bismuth molybdates are important catalysts for partial oxidation/ammoxidation of alkenes and other hydrocarbons (1, 2). Bismuth tungstates have also been examined as cat-

alysts for the oxidation and ammoxidation of unsaturated hydrocarbons, but they are not as catalytically active as their molybdate counterparts in spite of the similarities in the structural chemistry of tungsten and molybdenum (3, 4). The tetragonal phases of thin-film bismuth vanadates and bismuth niobates are efficient photoconductors (5). Thin-film bismuth molybdates have been found to be effective gas sensors for alcohols and ketones and may be used as Breathalyzer devices (6).

Selective oxidation/ammoxidation of propylene has received much attention due to the commercial importance of acrolein/acrylonitrile. A complex multicomponent catalyst with bismuth and molybdenum as the main components is used in industry for the propylene oxidation reaction. However, the research efforts have primarily focused on bismuth molybdates because these catalysts are thought to behave in the same manner as the industrial catalysts and they are much easier to prepare and characterize compared to their multicomponent industrial counterparts (7).

It is generally accepted that the first step in the partial oxidation of propylene over a bismuth molybdate catalyst is the abstraction of an α -hydrogen to form a symmetric allyl intermediate at the surface of the catalyst. This step is rate limiting above $\sim 400^\circ\text{C}$ as long as there is sufficient oxygen present (7–15). If the temperature is below 400°C , or if there is a deficiency of oxygen in the feed to the reactor, one of the catalyst reoxidation steps becomes the rate limiting step (7–15). Different mechanisms have been proposed for the ammoxidation of propylene (see Table 1) due to lack of information about the surface properties of bismuth molybdate catalysts (14). It is evident from Table 1 that there is a lack of agreement among various investigators about the roles of the individual components of the catalyst. Matsuura and co-workers, based on low temperature adsorption studies, attributes chemisorption and first hydrogen abstraction to Mo sites (16–19). Haber and co-workers' mechanism, based on *in situ* generation of allylic intermediate, proposes Bi sites to be responsible for chemisorption and first hydrogen abstraction (20, 21). Sleight and co-workers (22, 23), based on the crystal chemistry and oxidation reaction mechanism studies with oxide catalysts containing the Scheelite

¹ To whom correspondence should be addressed.

TABLE 1

Mechanisms for Propylene Ammoxidation in the Literature

Step	Matsuura	Haber	Sleight	Grasselli <i>et al.</i>
Olefin chemisorption	Mo (B site)	Bi	Mo	Mo
NH ₃ Chemisorption	Mo (B site)	Mo	Mo	Mo
NH formation				
1st allylic H abstraction	Mo (B site)	Bi	Mo	Bi
2nd (3rd) H abstractions	Mo (B site)	Mo	Mo	Mo
O(NH) insertion	Mo (A site)	Mo	Mo	Mo

structure, attribute all the reaction steps to tetrahedral Mo sites while Bi supplies an overlapping Bi/Mo conduction band ($6p/4d$) which serves as an electron sink. They further conclude that a molybdate is the actual site for allyl formation and that bismuth is not required for this step. Olefin oxidation uses the lattice oxygen which is rapidly replenished by the gaseous oxygen and bismuth promotes the high mobility of oxygen anions and probably serves as the actual site of oxygen adsorption. Grasselli and co-workers' mechanism proposes that chemisorption occurs on Mo sites and initial hydrogen abstraction occurs on Bi sites (24). This mechanism is based on a consideration of the reactions of both propylene, which is incorporated in the mechanism of the rate-determining step, and the allylic intermediate, independently generated *in situ* from allyl radical or allyl alcohol, which provide information concerning the steps after initial α -hydrogen abstraction.

A great deal of work has been done to determine the bulk properties of bismuth–metal oxide catalysts and different spectroscopic techniques have been utilized to characterize these catalysts. All bulk spectroscopic techniques (e.g., infrared, Raman, EXAFS, XANES) will only provide bulk structural information due to the extremely low surface areas of these oxides (typically ~ 0.1 to 1.0 m²/g). The small contribution of the surface component to the spectroscopy signal will generally be overshadowed by the significantly stronger contribution of the bulk component. Keulks and co-workers (25) studied the bismuth molybdate catalysts using infrared and Raman spectroscopies to determine the participation of the lattice oxygen in the selective oxidation reaction. Shifts in the vibrational bands after these catalysts were used for the oxidation of propylene with ¹⁸O₂ in the feed gas were interpreted as participation of all types of lattice oxygen ions in propylene oxidation. Grasselli (26), based on *in situ* Raman studies, concluded that there are different kinds of oxygen present in the bismuth molybdate catalyst. The oxygen associated with bismuth is chemically different from the oxygen bonded to molybdenum, and there may be oxygen bonded to both a bismuth and a molybdenum atom. It has been found

that oxygen involved in the first hydrogen abstraction is different from the oxygen which facilitates the second hydrogen abstraction. X-ray diffraction and Auger electron spectroscopy were used by Keulks and co-workers (27) to study the reoxidation of a γ -phase catalyst in order to monitor the oxidation states of bismuth and molybdenum. They concluded that reoxidation of bismuth vacancies takes place via transfer of oxygen from molybdenum, which can be rate limiting.

Most of the surface spectroscopies (e.g., X-ray photoelectron spectroscopy (XPS) Auger electron spectroscopy (AES), and ion scattering spectroscopy (ISS)), unfortunately, are not molecular in nature and cannot provide surface structural information. For example, X-ray photoelectron spectroscopy can only provide information about the surface composition and oxidation states of the surface components in the near surface region since the surface information is averaged over an escape depth of approximately 30–50 Å. Gryzbowska *et al.* (28) studied the reduction of bismuth molybdate catalysts in a hydrogen environment using XPS and UPS. The first step in the reduction of a fully oxidized catalyst was observed to be the reduction of Mo⁶⁺ to Mo⁴⁺. The reduction of Bi³⁺ to Bi⁰ was observed only after a majority of molybdenum had been reduced to Mo⁴⁺. However, very little is known about the outermost layer of bulk metal oxides and essentially no molecular level structural information is available about this last layer from XPS. Consequently, most of the researchers have assumed the last layer to be just an extension of the bulk structure and composition. In order to better understand the molecular structure–reactivity relationships and the role of different components in the bismuth–metal oxide catalysts it is imperative to explore the surface characteristics of these catalysts.

A related surface issue is whether it is possible to form two-dimensional metal oxide overlayers on bismuth–metal oxide catalysts. The activity of bismuth–metal oxide catalysts could possibly be increased by forming two-dimensional metal oxide overlayers of vanadia, molybdenum oxide, niobia, and tungsten oxide on a bismuth oxide support. These metal oxides readily form overlayers on supports like titania, zirconia, and alumina and generally have been found to be much more active compared to their corresponding bulk metal oxide catalysts. For instance, vanadia supported on titania is 100 times more active compared to bulk V₂O₅ crystals (29). Thus, the supports play an important role in activating the metal oxide overlayers for selective oxidation reactions (29, 30). Therefore, it is important to establish if supported metal oxide catalysts with vanadia, molybdenum oxide, niobia, and tungsten oxide present as surface phases on a bismuth oxide support can be synthesized. Such information will assist in developing a better understanding of the surface aspects of conventional bismuth–metal oxide catalysts.

This investigation was divided into two parts. In the first part of this study conventionally prepared bulk bismuth-metal oxide catalysts were studied for their structure, surface area, surface composition, and reactivity/selectivity in order to determine if there is a relationship between the bulk structures and their activity for methanol oxidation. The surface composition of the conventional bismuth-metal oxide catalysts was analyzed using X-ray photoelectron spectroscopy and compared with the activity of these catalysts for methanol oxidation. In the second part of this study, an attempt was made to synthesize model two-dimensional metal oxide overlayers of vanadia, molybdenum oxide, niobia, and tungsten oxide on a bismuth oxide support. The structure and activity of these model bismuth oxide supported metal oxides were compared with those of the conventional bulk bismuth-metal oxide catalysts. The surface of the model bismuth oxide supported metal oxide catalysts was also examined by XPS to determine the influence of the surface composition upon the activity/selectivity properties of the catalysts. The current studies demonstrate that these model bismuth oxide supported metal oxide catalyst studies provide additional insight into the structure-reactivity relationships of conventional bismuth-metal oxide catalysts.

EXPERIMENTAL

Catalyst Preparation

Conventional bulk bismuth-metal oxides. Conventional bulk bismuth-metal oxides like bismuth vanadates, bismuth molybdates, bismuth tungstates, and bismuth niobates had been previously prepared and characterized using Raman spectroscopy, and their bulk structures were determined prior to this study (4, 31, 32). Different compositions of bismuth vanadates, bismuth molybdates, bismuth tungstates, and bismuth niobates were prepared by mixing stoichiometric amounts of α - Bi_2O_3 (99.9%) with MoO_3 (99.9%), V_2O_5 (99.6%), Nb_2O_3 (99.9%), and WO_3 (99.9%), respectively. The resultant mixture was ground in acetone with agate mortar and pestal, and dried in air. All samples except bismuth vanadates were then calcined at 840°C in a flow of pure oxygen. Bismuth vanadates were calcined at 825°C in flowing oxygen. Further details about the preparation method can be found elsewhere (33, 34).

Model bismuth-metal oxides. In order to sufficiently characterize the model two-dimensional metal oxide overlayers on bismuth oxide, the bismuth oxide support should possess a significant surface area since the amount of metal oxide in the overlayer is proportional to the surface area. This is crucial for enhancing the surface signal of the metal oxide overlayers which otherwise may be too weak. For instance, the surface area of the support should be on the order of 10 m²/g in order to accommodate approximately 1 wt% loading of the supported metal oxides (30). The com-

mercially obtained bismuth oxide (Aldrich, 99.9% purity) was found to have too low a surface area, ~ 0.15 m²/g, due to its previous treatment at high calcination temperatures. Consequently, the surface area of bismuth oxide was increased by dissolution and recrystallization as described below.

The commercial bismuth oxide was dissolved in oxalic acid (Fisher Scientific, UN1759) to produce bismuth oxalate by stirring it for 3 h. The pH of the solution was then changed by adding NH_4OH (Fisher Scientific, NA2672) and the resulting precipitates were collected, filtered, and dried at 120°C overnight. The resulting powder was calcined at 300°C to decompose the bismuth oxalate as well as oxalic acid and ammonia. The surface area of the resulting bismuth oxide was found to be 5–6 m²/g. Several different batches of such high surface area bismuth oxide needed to be prepared because of the low solubility of bismuth oxide in oxalic acid. The Raman spectrum of each batch was taken and the same peaks (corresponding to α - Bi_2O_3) were observed for each preparation. This high surface area bismuth oxide was used as the support to prepare monolayer equivalent amounts of the metal oxide overlayers.

0.4 wt% $\text{V}_2\text{O}_5/\text{Bi}_2\text{O}_3$ ($\text{Bi}/\text{V} = 97$). This catalyst was prepared employing the incipient wetness impregnation method. The vanadia precursor was vanadium tri-isopropoxide oxide (Alfa, 95–98% purity) and the solvent was methanol (Fisher, certified ACS, 99.9% pure). Ammonium metavanadate, NH_4VO_3 , was not employed because of the low solubility of this salt in aqueous solutions. A solution of known amounts of the precursor and the solvent, corresponding to the incipient wetness impregnation volume and the final amount of vanadia required, was prepared in a glove box under a nitrogen atmosphere. The moisture and air-sensitive nature of vanadium tri-isopropoxide oxide required the preparation to be performed under a nitrogen environment. The solutions of the vanadia precursor and methanol were then thoroughly mixed with the bismuth oxide support, dried overnight at room temperature, and subsequently heated at 120°C overnight in flowing nitrogen. The sample was subsequently calcined at 300°C for 3 h, 400°C for 1 h, 500°C for 1 h, and 650°C for 1 h.

0.5 wt% $\text{MoO}_3/\text{Bi}_2\text{O}_3$ ($\text{Bi}/\text{Mo} = 123$). The molybdenum oxide precursor was ammonium heptamolybdate (Alfa products) and distilled water was used as the solvent. The method of preparation was the same as described above except that the preparation was performed in an ambient environment since the precursor did not require an inert environment. The catalyst was dried at 120°C overnight, and subsequently calcined at 300°C for 2 h, 400°C for 1 h, 500°C for 1 h and 650°C for 1.

0.6 wt% $\text{WO}_3/\text{Bi}_2\text{O}_3$ ($\text{Bi}/\text{W} = 166$). Ammonium tungstate (Pfaltz & Bauer, 99.9% purity) was employed as the precursor with distilled water as the solvent in the

preparation of this catalyst. The rest of the procedure was the same as described above.

0.6 wt% Nb_2O_5/Bi_2O_3 ($Bi/Nb = 95$). This catalyst was prepared using niobium oxalate (Pfaltz & Bauer) as the precursor and distilled water was used as the solvent. The rest of the procedure was the same as described above.

A second set containing high loadings of metal oxides (4Bi:1V, 3Bi:1Mo, 4Bi:1W, and 4Bi:1Nb) was also prepared to determine if the metal oxides in excess of monolayer equivalent amounts will form crystallites (V_2O_5 , MoO_3 , WO_3 , or Nb_2O_5) or will react with the bismuth oxide support to form compounds. These high loading catalysts would also allow for comparison with the conventional bulk bismuth–metal oxide catalysts previously reported in the literature. All these catalysts were dried at 120°C and then calcined at 300°C for 2 h, 400°C for 1 h, 500°C for 1 h, and 840°C for 1 h.

Characterization

Raman spectra of the samples were generated with a Spectra-Physics Ar^+ laser (model 171) by utilizing about 10–40 mW of the 514.5 nm beam for excitation. The scattered radiation from the sample was sent into a Spex Triplemate Spectrometer (Model 1877) which was coupled to an intensified photodiode array and optical multichannel analyzer (OMA III: Princeton Applied Research, model 1463). The photodiode array was thermoelectrically cooled to $-35^\circ C$. The Raman spectra were collected and recorded using an OMA III dedicated computer and software. The spectral resolution and reproducibility was experimentally determined to be better than 2 cm^{-1} . About 100–200 mg of each sample was pressed into a thin wafer of about 1 mm thickness. Each sample was mounted onto a spinning sample holder (~ 2000 rpm) where a 90° scattering geometry was used. Further details concerning the optical arrangements used in Raman experiments are described elsewhere (35).

The *in situ* Raman spectra were generated using a similar arrangement. The sample was rotated in a specially designed quartz glass cell at an angle ($\sim 45^\circ$) to the incident laser beam such that the reflected light was directed into the spectrometer. The *in situ* cell could be heated to different temperatures and different gaseous environments. In one set of experiments the samples were heated to different temperatures in flowing oxygen (Linde Gas, ultra high purity, hydrocarbon free) before taking the spectrum. In the second set of *in situ* experiments different combinations of oxygen, helium, and methanol (as specified in the text) were passed over the catalysts at 280°C with a total flow rate of ~ 100 standard cubic centimeter per minute (sccm).

The near-surface compositions of the bismuth molybdates, bismuth vanadates, bismuth tungstates, and bismuth niobates were investigated using X-ray photoelectron spectroscopy (XPS). An X-ray beam of predominantly MgK_{α}

or AlK_{α} X-rays was used for this study. The electron spectrometer was operated in the fixed analyzer transmission (FAT) mode. The specimens for XPS analysis were prepared by pressing the catalyst powder between a stainless steel holder and a polished single crystal silicon wafer. The powders adhered to the stainless steel holders without requiring additional adhesive materials and possessed relatively flat surfaces. After mounting, the holders were transferred to a turbomolecular pumped airlock. The airlock was evacuated to a pressure of 1×10^{-7} Torr. The holder was then installed in the vacuum chamber of a Model DS800 XPS surface analysis system manufactured by Kratos Analytical Plc, Manchester, UK. The chamber was evacuated to a base pressure of 5×10^{-9} Torr. A hemispherical electron energy analyzer was used for electron detection.

Catalysis Studies

The methanol oxidation reaction was used as a probe reaction to examine the catalysts for their relative activity and selectivity because of its sensitivity to different kinds of sites (29, 36–40). Redox sites (sites capable of being reduced and oxidized) yield formaldehyde, methyl formate, and dimethoxy methane; surface acid sites (Lewis as well as Brønsted) form dimethyl ether; and surface basic sites result in the formation of CO/CO₂ as the reaction product. The reaction was carried out in an isothermal fixed-bed differential reactor at atmospheric pressure and 280°C. The reactor was vertical and made of 6 mm. o.d. Pyrex glass tube. The catalyst was held in the middle of the tube between two layers of quartz wool. The feed gas flow was from top to bottom. The temperature around the reactor was maintained by a furnace (Linberg) connected to a temperature controller (Eurotherm). A mixture of helium (Linde, ultra high purity) and oxygen (Linde, ultra high purity) from two mass flow controllers (Brooks) were bubbled through a methanol (Fisher Scientific, 99.9% pure) saturator operating at $\sim 9.5^\circ C$ cooled by the flowing water from a cooler (Neslab RTE 110) to obtain a mixture of methanol, oxygen, and helium in a ratio of 6/11/83 (molar %) and a total flow rate of ~ 60 sccm. Pretreatment of the catalyst sample was done at 300°C for 30 min in a stream of oxygen and helium prior to each run. Blank experiments without a catalyst were performed to check for the reactivity of the glass tube and the quartz wool, and verified their inactivity. About 0.008–0.015 g of the catalyst was employed in order to maintain the conversion below 10% and the low reactivity of the catalysts assured the absence of mass and heat transfer limitations. The reaction is zero order with respect to oxygen due to the presence of excess oxygen in the feed. The outlet stream from the reactor to the gas chromatograph was heated to 120–130°C in order to avoid any condensation of the products. The reaction products were analyzed with an on-line gas chromatograph (HP 5840a) using two TCD's and an FID with two packed columns

(Porapak R and Carbosieve SII). The activities and selectivities are reported as initial values.

RESULTS

Conventional Bulk Metal Oxides

The Raman spectra of the conventional bismuth-metal oxides (Bi-M) were previously reported by Hardcastle *et al.* (4, 31, 32) and will be summarized in the Discussion section. The Raman spectra of the promoted bismuth molybdates ($\text{Bi}_{1.67}\text{Ce}_{0.25}\text{MoO}_6$, $\text{Bi}_{1.67}\text{Pr}_{0.25}\text{MoO}_6$, and $\text{Bi}_{1.67}\text{La}_{0.33}\text{MoO}_6$) were obtained in the current investigation and found to be similar to that of γ' - Bi_2MoO_6 . Consequently, molybdenum oxide possesses a tetrahedral structure in these compounds.

XPS results. The atomic surface concentrations of Bi, V, and Mo in bismuth vanadates and bismuth molybdates were determined by XPS. The relationships between the bulk Bi/M ($M = \text{Mo}, \text{V}$) ratios and the near surface Bi/M ratios are plotted in Figs. 1 and 2. The surface Bi/V ratio increases linearly with increasing bulk Bi/V ratio and is always greater than the corresponding bulk ratio in all the bismuth vanadate samples and suggests that there is bismuth enrichment at the surface. This conclusion is substantiated by the 60Bi:1V sample where only a trace amount of vanadium is barely detected on the surface. The XPS Bi/V ratio did not vary significantly with surface area. In the case of bismuth molybdates, the surface Bi/Mo ratio also increases linearly with increasing bulk Bi/Mo ratio, however, both ratios are comparable for most compositions (slope ~ 1).

Catalysis results. The normalized activity (moles of methanol converted/h \cdot m²) and selectivity data for the conventional bismuth vanadates and bismuth molybdates during methanol oxidation are reported in Tables 2 and 3. The specific surface areas for different compositions of bismuth vanadates and bismuth molybdates are also included

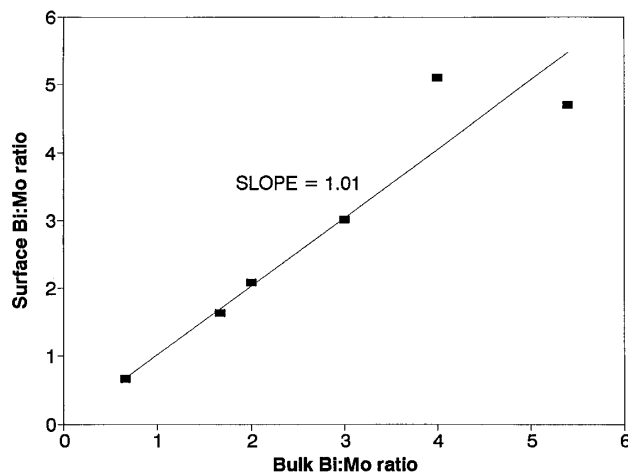


FIG. 2. XPS results of conventional bismuth molybdates.

in Tables 2 and 3. All compositions of bismuth vanadates calcined at high temperature (825°C) possess low surface areas and the 1Bi:1V sample calcined at 620°C has a surface area of 10.9 m²/g. The surface area of this catalyst decreases to 0.1 m²/g when calcined at 825°C. The major reaction product for the bismuth vanadates catalysts is formaldehyde regardless of bismuth vanadate composition (selectivity in the range of 72–93%) or surface area (two orders of magnitude), and the combustion product CO₂ is next in abundance. The selectivity toward dimethyl ether for the 6Bi:1V and 1Bi:1V compositions calcined at 825°C is attributed to acidic impurities or sites present in these catalysts which, however, could not be detected in the XPS analysis. The normalized activity does not vary with catalyst surface area, see 1Bi:1V catalyst, but varies by a factor

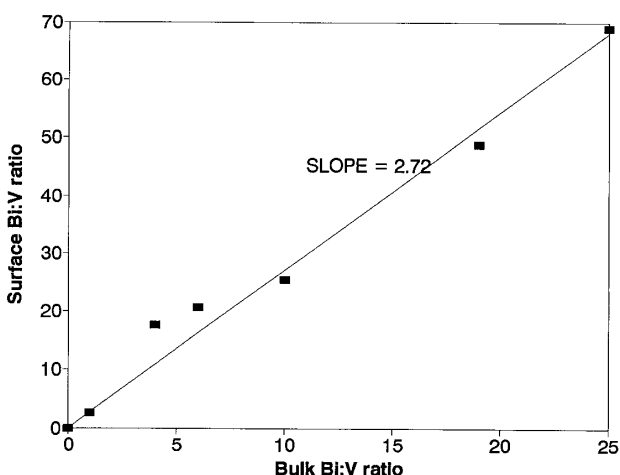


FIG. 1. XPS results of conventional bismuth vanadates.

TABLE 2

Catalysis Results of Bismuth Vanadates for Methanol Oxidation Reaction

Catalyst	S.A. ^a (m ² /g)	Activity ^b (mol/h \cdot m ²)	Selectivity % ^c			
			CO ₂	FM	DME	CO
1Bi:1V ^d	10.9	2.9×10^{-3}	9.9	89.8	0.3	—
1Bi:1V ^e	0.1	3.0×10^{-3}	12.0	83.8	4.2	—
4Bi:1V	0.2	6.0×10^{-3}	12.0	88.0	—	—
6Bi:1V	0.1	10×10^{-3}	17.5	72.0	10.5	—
10Bi:1V	0.4	2.8×10^{-3}	7.0	93.0	—	—
19Bi:1V	0.2	10×10^{-3}	6.9	93.1	—	—
25Bi:1V	0.1	13×10^{-3}	9.5	90.5	—	—
60Bi:1V	0.2	9.5×10^{-3}	7.2	92.8	—	—
Bi ₂ O ₃	0.1	18×10^{-3}	34.0	—	—	66.0

^a S.A. = surface area.

^b Reaction temperature is 280°C.

^c FM = formaldehyde, DME = dimethyl ether.

^d Calcination temperature is 620°C.

^e Calcination temperature is 825°C.

TABLE 3
Catalysis Results of Bismuth Molybdates for Methanol Oxidation Reaction

Catalyst	S.A. (m ² /g)	Activity (mol/h · m ²)	Selectivity % ^a				
			CO ₂	FM	DME	DMM	CO
α-Bi ₂ Mo ₃ O ₁₂	1.2	31.9 × 10 ⁻³	0.4	97.2	1.7	0.7	—
β-Bi ₂ Mo ₂ O ₉	1.7	2.3 × 10 ⁻³	0.6	97.8	1.6	—	—
γ-Bi ₂ MoO ₆	2.4	25.8 × 10 ⁻³	32.5	62.2	0.6	—	4.7
γ'-Bi ₂ MoO ₆	0.1	29 × 10 ⁻³	7.0	93.0	—	—	—
Bi ₃₈ Mo ₇ O ₇₈	<0.1	>4 × 10 ⁻³	13.0	58.0	—	—	29.0
Bi _{1.67} Ce _{0.25} MoO ₆	0.5	11 × 10 ⁻³	1.6	94.5	3.9	—	—
Bi _{1.67} Pr _{0.25} MoO ₆	0.1	37 × 10 ⁻³	1.5	93.0	3.5	—	2.0
Bi _{1.67} La _{0.33} MoO ₆	0.2	25.5 × 10 ⁻³	30.0	70.0	—	—	—
Bi ₂ O ₃	0.1	18 × 10 ⁻³	34.0	—	—	—	66.0

^a FM = formaldehyde, DME = dimethyl ether, DMM = dimethoxy methane.

of ~3–4 as the Bi/V ratio is varied. The minor activity variation with the Bi/V ratio appears to be random, possibly associated with experimental error, rather than systematic changes. Pure bismuth oxide calcined at 840°C possesses a slightly higher normalized activity, however, it is unselective to formaldehyde and produces only combustion products.

The normalized activities for several of the bismuth molybdates are somewhat higher than the bismuth vanadates and the activities do not appear to vary systematically with Bi/Mo ratio. Almost all compositions of bismuth molybdates show high selectivity (in the range of 58–98%) toward formaldehyde, which is formed from a redox site. All the bismuth molybdates produce small quantities of total oxidation product CO₂ and some of them form very small amounts of dimethyl ether which is due to the acidic sites (possibly related to some impurities). Addition of promoters like Ce, Pr, and La does not seem to have a significant effect on the normalized activity and selectivity of the bismuth molybdates containing the γ'-Bi₂MoO₆ structure. The addition of La does, however, decrease the formaldehyde selectivity.

Model Bismuth–Metal Oxide Catalysts

Raman spectroscopy results. The Raman spectra of the model bismuth–metal oxide catalysts are shown in Figs. 3–8. The ambient Raman spectra of the 0.4% V₂O₅/Bi₂O₃ sample as a function of calcination temperature are shown in Fig. 3. Spectrum 3a is for the pure bismuth oxide support which was used to prepare this catalyst. There is a broad carbonate band present at ~1063 cm⁻¹. The Raman spectrum of the 120°C dried sample exhibits a very broad and weak Raman band centered at ~880 cm⁻¹ arising from vanadium oxygen vibrations. A strong vanadia Raman band is observed at 300°C and higher temperatures. This Raman band shifts from 833 to 781 cm⁻¹ and becomes sharper with increasing calcination temperature.

Raman experiments were also performed under dehydrated conditions in order to obtain additional insights into this system. The Raman spectra of the 0.4% V₂O₅/Bi₂O₃ sample, originally calcined at 300°C, and obtained under dehydrated conditions are presented in Fig. 4 as a function of calcination temperature in the *in situ* cell. The vanadia Raman peak does not shift to any significant extent upon dehydration with increasing temperature and the carbonate signal is still present. It has been shown (41–43) that a tetrahedral coordinated surface vanadium oxide species on different oxide supports contain one terminal V=O bond and three bridging V–O–S bonds which give rise to a sharp Raman band in the 1015–1040 cm⁻¹ range under *in situ* conditions. However, for the *in situ* Raman spectra of the model 0.4% V₂O₅/Bi₂O₃ sample there is no band present in the 1015–1040 cm⁻¹ range confirming the absence of surface vanadia species and the Raman band at 833–781 cm⁻¹ was previously observed for bulk bismuth vanadate compounds (31). Furthermore, the sharpening of the Raman features

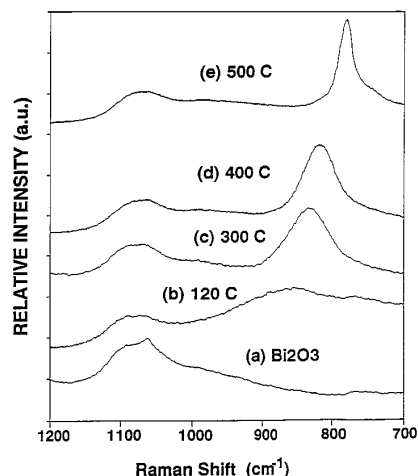


FIG. 3. Ambient Raman spectra of the 0.4% V₂O₅/Bi₂O₃ sample.

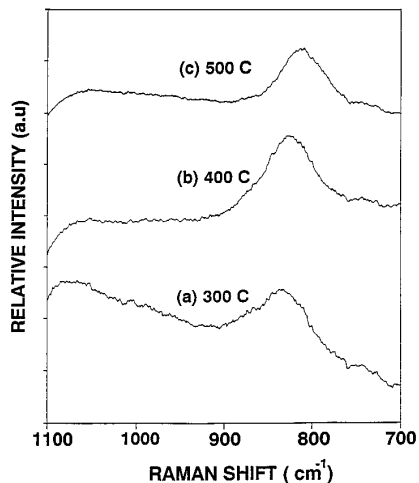


FIG. 4. *In situ* Raman spectra of the 0.4% V_2O_5/Bi_2O_3 sample under dehydrated conditions.

with increasing calcination temperature is due to the sample becoming more ordered or crystalline upon heating (Fig. 3).

The ambient Raman spectra of the 0.5% MoO_3/Bi_2O_3 catalyst as a function of calcination temperature are shown in Fig. 5. Spectrum 5a is for the pure bismuth oxide used as the support for this catalyst and the broad peak at $\sim 1063\text{ cm}^{-1}$ is due to the carbonate species. The dried sample hardly gives a signal due to molybdenum oxide in the $800\text{--}900\text{ cm}^{-1}$ region, but a strong peak appears at 874 cm^{-1} for the samples calcined at 300°C and above. The Raman band at $\sim 874\text{ cm}^{-1}$ does not shift in position but sharpens with increasing calcination temperature. The *in situ* Raman spectra for the sample originally calcined at 300°C are presented in Fig. 6 as a function of temperature in the *in situ* cell. There is a sharp carbonate band at 1063 cm^{-1} at 300 and 400°C which disappears at 500°C . Similar to the ambient spectra, the 874 cm^{-1} band does not shift to higher

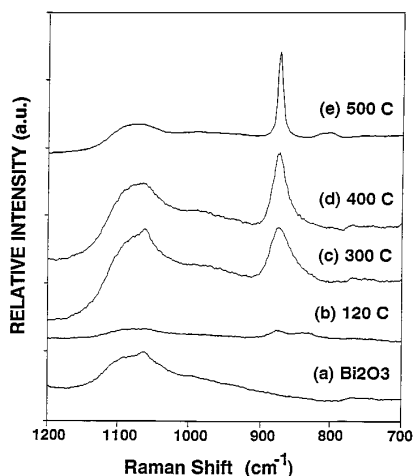


FIG. 5. Ambient Raman spectra of the 0.5% MoO_3/Bi_2O_3 sample.

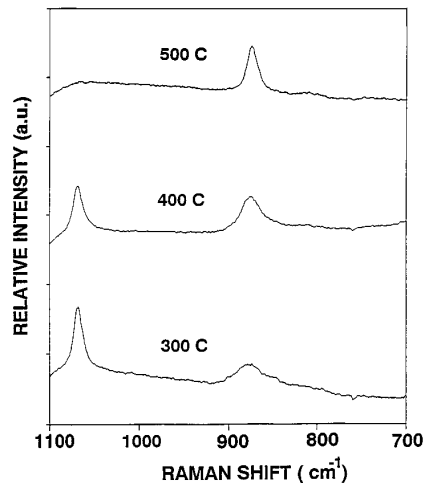


FIG. 6. *In situ* Raman Spectra of the 0.5% MoO_3/Bi_2O_3 sample under dehydrated conditions.

wave numbers but gets sharper with increasing calcination temperature. Surface molybdenum oxide species on different oxide supports give rise to a Raman band in the $976\text{--}1008\text{ cm}^{-1}$ range under *in situ* conditions (30, 43). This band is not present for the *in situ* Raman spectrum of 0.5% MoO_3/Bi_2O_3 , which suggests that surface molybdenum oxide species are not present on the bismuth oxide surface. The Raman band at $\sim 874\text{ cm}^{-1}$ was previously observed for bulk bismuth molybdate compounds (32). The crystallization of bismuth molybdate with increasing temperature accounts for the sharpening of the Raman band at 874 cm^{-1} (see Fig. 5). The same conclusion was made in the case of low loadings of tungsten oxide and niobia on the bismuth oxide support. Thus, surface metal oxide species of vanadia, molybdenum oxide, tungsten oxide, and niobia are not stable as metal oxide overlayers on bismuth oxide and form bulk bismuth-metal oxide compounds upon heating.

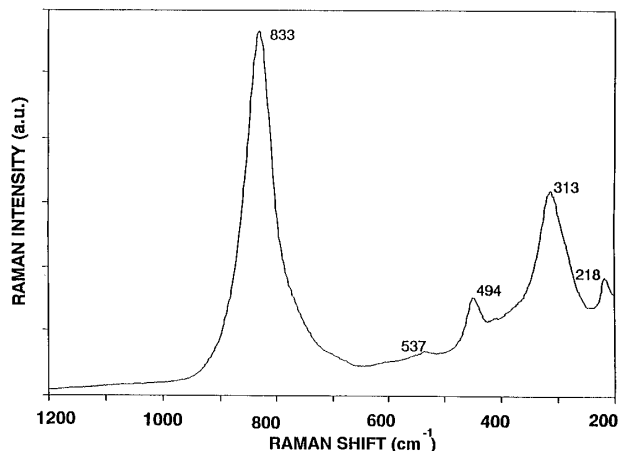


FIG. 7. Ambient Raman spectra of the 4Bi:1V model catalyst.

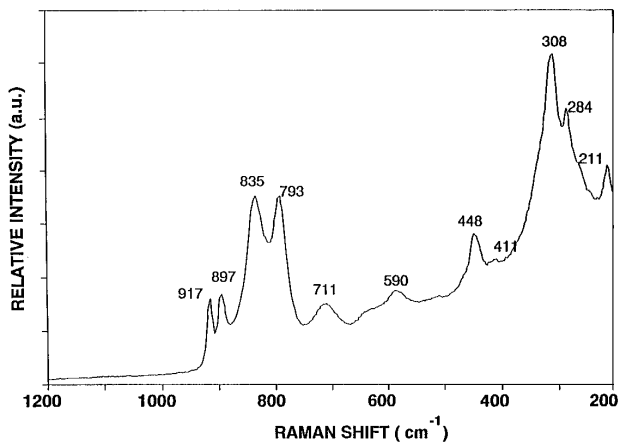


FIG. 8. Ambient Raman spectra of the 4Bi:1W model catalyst.

Two representative ambient Raman spectra of high loading samples (Bi:V=4:1 and Bi:W=4:1) calcined at 500°C are shown in Figs. 7 and 8. Typically when the vanadia loading is increased on oxide supports beyond monolayer coverage it results in the formation of V_2O_5 crystals with a sharp Raman band at 994 cm^{-1} (44). However, the resultant spectrum of the high loading sample is the same as the conventional bulk bismuth vanadate (Bi:V=4:1) spectrum obtained by Hardcastle *et al.* (31). Thus, it appears that the vanadium oxide is not present as crystalline V_2O_5 on the bismuth oxide support because it strongly interacts with bismuth oxide due to the reaction between the basic bismuth oxide and acidic vanadium oxide components. Secondly, there is no effect of the preparation method on the structure of the catalyst and both methods (physical mixing and incipient wetness impregnation) give the same product as far as the structure of this bismuth vanadate is concerned. The same is true for high loadings of molybdenum oxide, tungsten oxide, and niobia on bismuth oxide since all these components do not form MoO_3 , WO_3 , and Nb_2O_5 crystallites.

XPS results. The XPS results of low loading and high loading metal oxide model catalysts are presented in Figs. 9 and 10, respectively. For the low loading catalysts, the Bi:M ($M=V, Mo, W, Nb$) XPS ratios were determined for the catalysts calcined at 300, 500, and 650°C. The Bi:M ratio increases with increasing calcination temperature for all the catalysts. The 0.4% V_2O_5/Bi_2O_5 catalyst possesses some vanadium at or near the surface at 650°C, whereas, all other low loading catalysts are found to have no molybdenum, tungsten, or niobium at the surface after calcination at 650°C. That is why the surface Bi:M ratio for these catalysts is shown to be approaching infinity (Fig. 9) after the 650°C calcination. For the high loading model catalysts, the Bi:M XPS ratios were determined after calcination of the catalysts at 300, 500, and 840°C. This ratio also increases

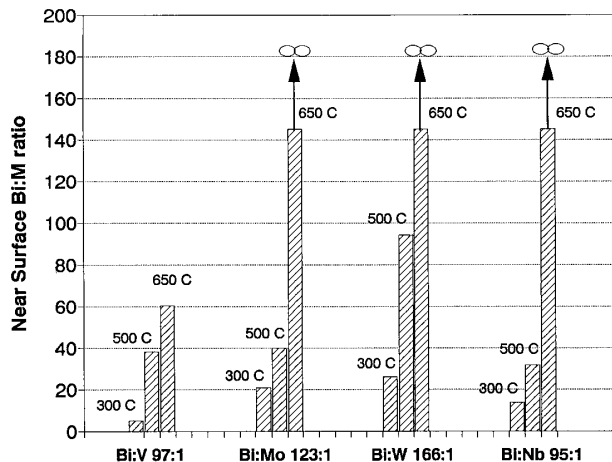


FIG. 9. XPS results of low loading model catalysts.

with increasing calcination temperature for all the catalysts as shown in Fig. 10.

Catalysis results. The methanol oxidation reaction was examined over the catalysts calcined at three different temperatures for both low loading and high loading metal oxide model catalysts. The results obtained are presented in Tables 4–9. These tables also contain the surface areas of these catalysts after different calcination temperatures. Conventional bulk bismuth–metal oxide catalysts are known to have low surface areas ($0.1\text{--}0.5\text{ m}^2/\text{g}$) and in this study the goal was to prepare high surface area catalysts using bismuth oxide and transition metal oxides. The bismuth oxide support used for preparing these catalysts had a surface area on the order of $5\text{--}6\text{ m}^2/\text{g}$. The surface areas of all the catalysts are significantly higher than the surface areas of conventional bulk bismuth–metal oxide catalysts after low calcination temperature, but as the calcination temperature is increased the surface areas of the model

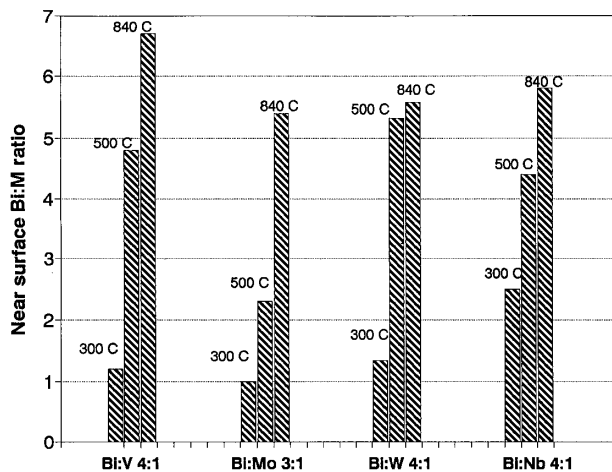


FIG. 10. XPS results of high loading model catalysts.

TABLE 4

Catalysis Results of Low Loading Model Catalysts for Methanol Oxidation Reaction (Calcination Temp. 300°C)

Catalyst	Activity (mol/h · m ²)	S.A. (m ² /g)	Selectivity %		
			CO ₂	HCHO	CO
0.4% V ₂ O ₅ /Bi ₂ O ₃	82.2 × 10 ⁻³	3.1	92.8	7.2	—
0.5% MoO ₃ /Bi ₂ O ₃	16.2 × 10 ⁻³	3.5	90.8	8.8	0.4
0.6% WO ₃ /Bi ₂ O ₃	16.0 × 10 ⁻³	3.8	85.4	14.6	—
0.6% Nb ₂ O ₅ /Bi ₂ O ₃	60.3 × 10 ⁻³	3.7	98.6	1.4	—
Bi ₂ O ₃	33.7 × 10 ⁻³	3.8	90.0	9.0	1.0

catalysts decrease. After high calcination temperature, the surface areas of the model catalysts become comparable to that of the bulk conventional catalysts.

For low metal oxide loadings and calcination at 300°C, the vanadia on Bi₂O₃ and the niobia on Bi₂O₃ catalysts possess comparable normalized activities, whereas, molybdenum oxide on Bi₂O₃ and tungsten oxide on Bi₂O₃ are somewhat less active. However, all four catalysts are very unselective to formaldehyde and give primarily combustion products (CO₂ and a trace of CO). Pure Bi₂O₃ (calcined at 300°C) also exhibits a comparable normalized activity and a low selectivity to formaldehyde. As the calcination temperature of these catalysts is increased to 500°C there is a decrease in surface area, but the normalized activities increase slightly (V, W, Nb) or remain about the same (Mo). However, the normalized activity for the pure bismuth oxide catalyst decrease significantly. The selectivity to formaldehyde significantly increases for all four bismuth oxide supported metal oxide catalysts as the calcination temperature is increased. The formaldehyde selectivity over the pure bismuth oxide support initially increases somewhat with the calcination temperature, but formaldehyde is not produced and only combustion products are observed after high calcination temperatures. The normalized activities further increase for the bismuth oxide supported metal oxide catalysts upon increasing the calcination temperature to 650°C (see Table 6). The selectivity toward formaldehyde also in-

TABLE 5

Catalysis Results of Low Loading Model Catalysts for Methanol Oxidation Reaction (Calcination Temp. 500°C)

Catalyst	Activity (mol/h · m ²)	S.A. (m ² /g)	Selectivity %		
			CO ₂	HCHO	CO
0.4% V ₂ O ₅ /Bi ₂ O ₃	122 × 10 ⁻³	1.8	80.3	19.1	0.6
0.5% MoO ₃ /Bi ₂ O ₃	13.8 × 10 ⁻³	2.9	76.9	20.5	2.6
0.6% WO ₃ /Bi ₂ O ₃	36.0 × 10 ⁻³	1.5	64.4	33.7	1.9
0.6% Nb ₂ O ₅ /Bi ₂ O ₃	73.4 × 10 ⁻³	1.8	96.6	2.9	0.5
Bi ₂ O ₃	14.7 × 10 ⁻³	1.7	82.0	18.0	1.0

TABLE 6

Catalysis Results of Low Loading Model Catalysts for Methanol Oxidation Reaction (Calcination Temp. 650°C)

Catalyst	Activity (mol/h · m ²)	S.A. (m ² /g)	Selectivity %		
			CO ₂	HCHO	CO
0.4% V ₂ O ₅ /Bi ₂ O ₃	197 × 10 ⁻³	0.4	41.8	58.2	—
0.5% MoO ₃ /Bi ₂ O ₃	48.0 × 10 ⁻³	0.5	18.6	81.4	—
0.6% WO ₃ /Bi ₂ O ₃	112 × 10 ⁻³	0.3	18.0	82.0	—
0.6% Nb ₂ O ₅ /Bi ₂ O ₃	147 × 10 ⁻³	0.4	53.1	46.9	—
Bi ₂ O ₃	8.3 × 10 ⁻³	0.4	36.4	—	63.6

creases with increasing calcination temperature for the bismuth oxide supported metal oxide catalysts. The normalized activity of pure bismuth oxide further decrease upon calcination at 650°C. Thus, the normalized activities and formaldehyde selectivities of the model bismuth oxide supported catalysts increase significantly with calcination temperature.

The catalysis results of the high metal oxide loading model catalysts calcined at different temperatures are shown in Tables 7–9. The normalized activities of the catalysts generally decreases with increasing calcination temperature with the exception of the Bi–Nb (4:1) catalyst. The selectivity toward formaldehyde also improves with the exception of bismuth niobate. The bismuth niobate catalyst produces deep combustion product (CO₂), regardless of the calcination temperature. In general, high loading catalysts are more selective to formaldehyde compared to the low loading catalysts. Therefore, the formaldehyde selectivity improves as a function of both the metal oxide loading on the bismuth oxide as well as the calcination temperature. However, pure bismuth oxide is unselective toward formaldehyde even after high temperature treatments and its normalized activity decreases with calcination temperature.

In situ Raman spectroscopy. Raman spectroscopy was performed on high loading Bi–M catalysts (4Bi:1W,

TABLE 7

Catalysis Results of High Loading Model Catalysts for Methanol Oxidation Reaction (Calcination Temp. 300°C)

Catalyst	Activity (mol/h · m ²)	S.A. (m ² /g)	Selectivity %			
			CO ₂	FM	DME	CO
Bi:V::4:1	4.2 × 10 ⁻³	4.9	31.4	67.9	0.7	—
Bi:Mo::3:1	21.2 × 10 ⁻³	5.0	4.2	95.2	—	0.6
Bi:W::4:1	9.8 × 10 ⁻³	3.2	63.2	31.6	5.2	—
Bi:Nb::4:1	62.8 × 10 ⁻³	3.9	100.0	—	—	—
Bi ₂ O ₃	33.7 × 10 ⁻³	3.8	90.0	9.0	—	1.0

TABLE 8

Catalysis Results of High Loading Model Catalysts for Methanol Oxidation Reaction (Calcination Temp. 500°C)

Catalyst	Activity (mol/h · m ²)	S.A. (m ² /g)	Selectivity %			
			CO ₂	FM	DME	CO
Bi:V::4:1	3.3 × 10 ⁻³	3.2	16.5	83.5	—	—
Bi:Mo::3:1	9.1 × 10 ⁻³	2.2	19.8	74.7	—	5.5
Bi:W::4:1	13.8 × 10 ⁻³	2.4	46.9	49.5	0.6	3.0
Bi:Nb::4:1	60.5 × 10 ⁻³	3.8	99.4	—	—	0.6
Bi ₂ O ₃	14.7 × 10 ⁻³	1.7	82.0	18.0	—	—

4Bi:1V, 3Bi:1Mo, 4Bi:1Nb) under *in situ* conditions of methanol reaction. It was observed that in the presence of methanol and oxygen with helium as the carrier gas (molar ratio of methanol/oxygen/helium ~4/20/76) no significant change in the Raman signal was observed. However, in the presence of methanol and helium (no oxygen present) a substantial reduction of the Raman bands was observed for all the Bi-M catalysts, which was also accompanied by darkening of the samples. No relationship was evident with the decrease in Raman intensity in the methanol/helium gas stream and the catalytic activity shown in Tables 7, 8, and 9.

DISCUSSION

Five distinct vanadium containing phases have been identified in conventional bismuth vanadates and the different phases are present in the conventional bismuth-metal oxide catalysts with varying bismuth to metal ratio (4, 31, 32, 34). Low bismuth to vanadium ratio catalysts (1Bi:1V and 4Bi:1V) possess BiVO₄ as the major phase (31). 6Bi:1V and 10Bi:1V catalysts have Type II (triclinic phase) and Type I (fluorite like cubic phase) as the major phases, respectively. γ -VO₄ in the sillenite structure is the predominant phase present in 19Bi:1V, 25Bi:1V, and 60Bi:1V catalysts. The vanadium oxide species are tetrahedrally coordinated in all of the bismuth vanadates and the degree of

TABLE 9

Catalysis Results of High Loading Model Catalysts for Methanol Oxidation Reaction (Calcination Temp. 840°C)

Catalyst	Activity (mol/h · m ²)	S.A. (m ² /g)	Selectivity %			
			CO ₂	FM	DME	CO
Bi:V::4:1	77 × 10 ⁻³	0.1	9.0	91.0	—	—
Bi:Mo::3:1	60.5 × 10 ⁻³	0.2	13.4	86.6	—	—
Bi:W::4:1	56 × 10 ⁻³	0.1	14.4	85.6	—	—
Bi:Nb::4:1	7.0 × 10 ⁻³	0.1	100.0	—	—	—
Bi ₂ O ₃	18 × 10 ⁻³	0.1	34.0	—	—	66.0

symmetry increases with increasing Bi:V ratio. The V-O bond distances for VO₄ tetrahedron decreases in the order γ -VO₄ > Type I > Type II > BiVO₄. In the case of bismuth molybdates, seven distinct molybdenum containing phases and four bismuth oxide phases were identified in different compositional regions (32). Molybdenum oxide possesses an octahedral structure in α -Bi₂Mo₃O₁₂ and γ -Bi₂MoO₆, whereas, it possesses a tetrahedral structure in β -Bi₂Mo₂O₉, γ' -Bi₂MoO₆, Bi₆Mo₂O₁₅, Bi₃₈Mo₇O₇₈, and Bi-Mo-O sillenite phases. The Bi₂O₃-Nb₂O₅ system contains five distinct bismuth niobate phases depending upon the Bi:Nb ratio (4). Niobia is found to have an octahedral structure in all of the bismuth niobate catalysts (4). However, as the Bi:Nb ratio is increased from 15:1 to 60:1 the NbO₆ octahedra of the Type I phase become progressively more distorted. There are three distinct bismuth tungstate phases present in the Bi₂O₃-WO₃ system of varying Bi:W ratio. Similar to molybdenum oxide, the structure of tungsten oxide in bismuth tungstates changes from octahedral to tetrahedral with increasing loading. In summary, the coordination of metal oxides in bismuth oxide compounds is a function of the type of the metal oxide and the Bi:M ratio.

The surface compositions of the conventional bismuth vanadate and molybdate catalysts were determined by XPS as a function of Bi/M ratio ($M = V, Mo, W, Nb$). The XPS surface analysis revealed a linear increase in the surface Bi/M ratios with increasing bulk Bi/M ratios. The slope for the bismuth vanadates was 2.7 suggesting an enrichment of bismuth in the surface region. However, at very high Bi/V ratios, e.g., 60, vanadium could not be detected in the surface region suggesting that for very dilute systems only bismuth may preferentially exist on the surface. For the bismuth molybdates the slope was approximately unity over the range investigated indicating a comparable concentration of molybdenum in the bulk and the surface region. The methanol oxidation studies over the conventional bismuth vanadate catalysts revealed that selectivity to formaldehyde was essentially independent of the Bi/V ratio as well as its surface area (over two orders of magnitude). The normalized activities varied somewhat (~3-4), but not in a systematic fashion. Consequently, the reactivity and selectivity of the bismuth vanadates for methanol oxidation to formaldehyde are not sensitive to the vanadia surface concentration as well as the specific vanadia structure present since the VO₄ tetrahedra became less distorted with increasing Bi/V ratios. The bismuth molybdates also generally yielded very high selectivities to formaldehyde and did not depend in any significant way upon the specific Mo coordination or the Mo surface concentration. Two catalysts that exhibited somewhat lower selectivities to formaldehyde and higher selectivities to carbon oxides were γ -Bi₂MoO₆, containing octahedral Mo species, and Bi₃₈Mo₇O₇₈, containing tetrahedral Mo species. The normalized activities for the bismuth molybdates varied by a factor of ~10, but not in a system-

atic fashion. Thus, the normalized reactivity and selectivity of the bismuth vanadate and bismuth molybdate catalysts were not related to the specific V or Mo structures as well as their surface concentrations.

The influence of promoters upon the γ' - Bi_2MoO_6 catalyst was also examined. Raman studies revealed that the promoters (Ce, Pr, and La) did not perturb the tetrahedral MoO_4 sites present in these bismuth molybdates. The methanol oxidation catalytic studies revealed that the catalytic activities of the promoted catalysts were essentially not influenced by the addition of the promoters even though the Bi/Mo ratio of the promoted catalysts were lower than in the unpromoted catalyst. As already mentioned above, the catalysts were generally more sensitive to the surface area than the specific Bi/Mo ratio. The addition of Ce and Pr also did not affect the selectivity to formaldehyde, but the addition of La did decrease the selectivity to formaldehyde from 93 to 70%. Brazdil *et al.* (45–47), however, found that addition of cerium to bismuth molybdate significantly enhanced its catalytic activity for the selective oxidation of propylene to acronitrile. They concluded that the multivalent redox couple formed by cerium enhances oxygen ion, electron, and anion vacancy transport in the solid, which enhances catalytic activity by increasing the reconstruction/reoxidation rate of the active Bi and Mo containing sites. This results in an effective increase of the number of active sites available at the surface at any given time. These results could be reaction specific since for methanol oxidation reaction there is no significant improvement in the catalytic results.

Additional insight into surface interactions in the bismuth–metal oxide systems were obtained from the model studies using a moderate surface area bismuth oxide support. The model studies clearly demonstrated that stable metal oxide (V, Mo, W, and Nb) overlayers cannot be formed on a bismuth oxide support and that the deposited metal oxides readily react with bismuth oxide to form bulk bismuth–metal oxide compounds. A model representing the evolution of the deposited metal oxide overlayers on a bismuth oxide support with temperature is shown in Fig. 11. The deposited metal oxides are relatively well dispersed upon drying to 120°C since strong Raman bands due to the crystalline bismuth–metal oxide phases are absent. However, heating to higher temperatures results in the appearance of strong Raman bands due to crystalline bismuth–metal oxide phases. These Raman bands become sharper with higher calcination temperatures, which is a consequence of the increased degree of crystallization and order in these bismuth–metal oxide phases at elevated temperatures. Furthermore, the Raman bands also shift to lower frequencies reflecting an increase in local Bi/M ratio with increasing calcination temperature due to incorporation of additional bismuth in the bismuth–metal oxide catalysts. This shifting in frequencies with increase in calcination tem-

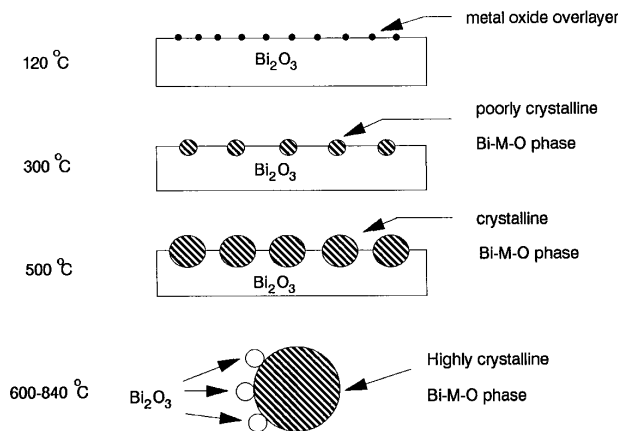


FIG. 11. Proposed model for the bismuth–metal oxide catalysts.

perature is especially true for the bismuth vanadate system, which is sensitive to the Bi/V ratio. The increase in the Bi/M ratio in the bismuth–metal oxide crystals is also reflected in the increase in the XPS surface Bi/M ratio with increasing calcination temperature. Eventually, at high temperatures the bismuth–metal oxide phase is the predominant phase with a high Bi/M ratio and only minor amounts of unreacted bismuth oxide phases remain. The amount of unreacted bismuth oxide remaining decreases with increasing metal oxide loading. The bismuth–metal oxide phases formed from the metal oxide overlayers on the bismuth oxide support are indistinguishable from the phases formed by previous methods such as physically grinding, mixing, and calcining the metal oxide components.

The selectivity patterns of these model bismuth–metal oxide compounds toward methanol oxidation to formaldehyde reveal that only highly crystalline phases formed at high calcination temperatures result in selective catalysts. Poorly crystalline bismuth–metal oxide phases formed at low calcination temperatures are not very selective for methanol oxidation and primarily yield combustion products. The normalized activities of poorly crystalline bismuth–metal oxide phases are also low and increase with calcination temperature. The requirement of highly crystalline bismuth–metal oxide phases may be related to the efficient transport of lattice oxygen during the redox cycle. Increasing the calcination temperature in the model bismuth–metal oxide catalysts also affects the surface area and the local Bi/M ratio. The methanol oxidation studies with the conventional bismuth–metal oxide catalysts demonstrated that the surface area does not affect the selectivity or the normalized catalyst reactivity. Machiels *et al.* (48), based on their kinetic studies for methanol oxidation with different molybdates, concluded that the reaction rate was nearly independent of oxygen partial pressure, except at very low pressures in the reactor in which case the catalyst begins to be reduced. However, the reaction rate had a positive

dependence on methanol partial pressure. It was also found that various bismuth molybdate phases that are well-known selective oxidation catalysts for other reactions are much less active for methanol oxidation (48). Our methanol oxidation studies with the conventional bismuth–metal oxide catalysts demonstrated that the Bi/*M* ratio generally does not affect the catalyst selectivity. Increasing the initial metal oxide loading in the model bismuth–metal oxide catalysts had a positive effect on the selectivity because it also enhanced the crystallization process. The current observations with the model bismuth–metal oxide catalysts account for the requirement of conventional bismuth–metal oxide catalysts to possess highly crystalline phases with corresponding low surface areas, in order to be selective oxidation catalysts.

The surface compositions of the outermost layer of the conventional bismuth–metal oxide catalysts are still not known from the current investigation since XPS only samples the near surface region (30–50 Å). This information could possibly be obtained with low energy ion scattering spectroscopy which tends to sample the outermost layers of catalysts. Such experiments need to be performed under *in situ* conditions after catalyst calcination and reduction treatments since surface carbonates are formed on samples exposed to ambient conditions. *In situ* Raman studies were inconclusive regarding the nature of the active site since the Raman features remained essentially unchanged. It is unlikely that any molecular structural information about the surface sites in the outermost layer will ever be obtained given the unusually low surface areas of the conventional bismuth–metal oxide catalysts since the molecular spectroscopies required for such measurements are inherently bulk techniques (Raman, IR, EXAFS/XANES, NMR, etc.). From the current investigation, however, it does appear that there is a tendency for bismuth to be enriched in the outermost layer of such catalysts under oxidizing conditions.

CONCLUSIONS

In order to understand the structure–reactivity relationship of an important class of bismuth–metal oxide catalysts, being used for various commercial reactions, model bismuth–metal oxide catalysts were prepared and physically and chemically characterized. The findings of this study demonstrated that vanadia, molybdenum oxide, tungsten oxide, and niobia cannot be supported as two-dimensional overlayers on a bismuth oxide support. These metal oxides react with the bismuth oxide and form a compound. The crystals of this compound, dispersed on the surface of the catalyst, grow when the catalysts are heated after drying at room temperature. Catalytic results indicate that these catalysts need to be calcined at a high temperature (~800°C) in order to make them selective for the

partial oxidation products because it was found that only highly crystalline bismuth–metal oxide phases are selective to formaldehyde. The catalysts calcined at low temperatures exhibit a poor selectivity toward formaldehyde. As the calcination temperature is increased, the surface area and the activity of these catalysts start decreasing, whereas the Bi: *M* ratio starts increasing. *In situ* Raman spectroscopy using methanol/oxygen/helium, methanol/helium, and oxygen/helium as reaction gasses do not reveal any additional information regarding the nature of the active site. There is no effect of the preparation method because the conventional catalysts, prepared by physical mixing, and the model catalysts, prepared by the incipient wetness impregnation technique, are shown to have similar structure and reactivity. The activity of conventional bismuth–metal oxide catalysts does not depend upon the bulk structure and the near surface composition, and is a function of the surface area of the catalytic material. The selectivity of conventional bismuth–metal oxide catalysts is not a function of the surface area, the surface composition, or the bulk structure.

ACKNOWLEDGMENTS

We are grateful to D. S. Kim for obtaining the catalytic data of the conventional bismuth vanadates. We are also indebted to D. A. Jefferson (University of Cambridge), D. A. Buttrey (University of Delaware), and J. M. Thomas (Royal Institute of Great Britain) for supplying the conventional bismuth molybdate samples. We gratefully acknowledge Professor J. Haber (Polish Academy of Science) for stimulating discussions.

REFERENCES

1. Thomas, J. M., Jefferson, D. A., and Millward, G. R., *JOEL News* **23E**, 7 (1985).
2. Jefferson, D. A., Thomas, J. M., Uppal, M. K., and Grasselli, R. K., *J. Chem. Soc. Chem. Commun.* 594 (1983).
3. Kolchin, I. K., Gal'perin, E. L., Bobokov, S. S., and Margolis, L. Y., *Neftekhimiya* **5**, 111 (1965).
4. Hardcastle, F. D., Ph.D. Dissertation, Lehigh University, 1990.
5. Sekiya, T., Tsuzuki, A., and Torii, Y., *Mater. Res. Bull.* **20**, 1383 (1985).
6. Hykaway, N., Sears, W. M., Frindt, R. F., and Morrison, S. R., *Sens. Actuators* **15**, 105 (1988).
7. Synder, T. P., and Hill, C. G., *Catal. Rev.-Sci. Eng.* **31**, 43 (1989).
8. Keulks, G. W., *J. Catal.* **19**, 232 (1970).
9. Wragg, R. D., Ashmore, P. G., and Hockey, J. A., *J. Catal.* **22**, 49 (1971).
10. Sancier, K. M., Wentreck, P. R., and Wise, H., *J. Catal.* **39**, 141 (1975).
11. Grasselli, K. M., *J. Chem. Educ.* **63**, 216 (1986).
12. Burrington, J. D., and Grasselli, R. K., *J. Catal.* **63**, 235 (1980).
13. Adams, C. R., and Jennings, T. J., *J. Catal.* **2**, 63 (1962).
14. Grasselli, R. K., and Burrington, J. D., in "Advances in Catalysis" (D. D. Eley, H. Pines, and P. B. Weisz, Eds.), Vol. 30, p. 133. Academic Press, Orlando, 1981.
15. Adams, C. R., and Jennings, T. J., *J. Catal.* **3**, 549 (1964).
16. Matsuura, I., *J. Catal.* **35**, 452 (1974).
17. Matsuura, I., *J. Catal.* **33**, 420 (1974).
18. Matsuura, I., and Schuit, G. C. A., *J. Catal.* **25**, 314 (1972).
19. Matsuura, I., and Schuit, G. C. A., *J. Catal.* **20**, 19 (1971).
20. Grzybowska, B., Haber, J., and Janas, J., *J. Catal.* **49**, 150 (1977).
21. Haber, J., and Grzybowska, B., *J. Catal.* **28**, 489 (1973).

22. Sleight, A. W., in "Advanced Materials in Catalysis" (J. J. Burton and R. L. Garten, Eds.), p. 181. Academic Press, New York, 1977.
23. Linn, W. J., and Sleight, A. W., *Ann. N.Y. Acad. Sci.* **272**, 22 (1976).
24. Burrington, J. D., Kartisek, C. T., and Grasselli, R. K., *J. Catal.* **63**, 235 (1980).
25. Hoefs, E. V., Monnier, J. R., and Keulks, G. W., *J. Catal.* **57**, 331 (1979).
26. Grasselli, R. K., *App. Catal.* **15**, 127 (1985).
27. Uda, T., Lin, T. T., and Keulks, G. W., *J. Catal.* **62**, 26 (1980).
28. Gryzbowska, B., Haber, J., Marczewski, W., and Ungier, L., *J. Catal.* **42**, 327 (1976).
29. Deo, G., and Wachs, I. E., *J. Catal.* **129**, 307 (1991).
30. Wachs, I. E., Deo, G., Kim, D. S., Vuurman, M. A., and Hu, H., in "Proceedings of 10th International Congress on Catalysis Budapest, 1992" (L. Guzzi, F. Solimosi, and P. Tetenyi, Eds.), Part B, p. 543. Akademiai Kiado, Budapest, 1993.
31. Hardcastle, F. D., Wachs, I. E., Ekerdt, H., and Jefferson, D. A., *J. Solid State Chem.* **90**, 194 (1991).
32. Hardcastle, F. D., and Wachs, I. E., *J. Phys. Chem.* **95**, 10763 (1991).
33. Zhou, W., *J. Solid State Chem.* **76**, 290 (1988).
34. Buttrey, D. J., Jefferson, D. A., and Thomas, J. M., *Mater. Res. Bull.* **21**, 739 (1986).
35. Wachs, I. E., Hardcastle, F. D., and Chan, S. S., *Spectroscopy* **1**(8), 30 (1986).
36. Tatibouet, J. M., Germain, J. E., and Volta, J. C., *J. Catal.* **82**, 240 (1983).
37. Ohuchi, F., Firment, L. E., Chowdhry, U., and Ferretti, A., *J. Vac. Sci. Technol. A* **2**, 1022 (1984).
38. Louis, C., Tatibouet, J. M., and Che, M., *J. Catal.* **68**, 464 (1981).
39. Segawa, K., Soeya, T., and Kim, D. S., *Sekiyu Gakkaishi (J. Jpn. Petrol. Inst.)* **33**, 347 (1990).
40. Roozeboom, F., Cordingley, P. D., and Gellings, P. J., *J. Catal.* **68**, 464 (1981).
41. Went, G., Oyama, S. T., and Bell, A. T., *J. Phys. Chem.* **94**, 4240 (1990).
42. Vuurman, M. A., Hirt, A. M., and Wachs, I. E., *J. Phys. Chem.* **95**, 9928 (1991).
43. Vuurman, M. A., and Wachs, I. E., *J. Phys. Chem.* **96**, 5008 (1992).
44. Deo, G., and Wachs, I. E., *J. Phys. Chem.* **95**, 5889 (1991).
45. Brazdil, J. F., and Grasselli, R. K., *J. Catal.* **79**, 104 (1983).
46. Brazdil, J. F., Glaeser, L. C., and Grasselli, R. K., *Phys. Chem.* **87**, 5485 (1983).
47. Brazdil, J. F., Teller, R. G., Grasselli, R. K., and Kostiner, E., in "Solid State Chemistry in Catalysis" (J. F. Brazdil, R. K. Grasselli, Eds.), ACS Symposium Series 279, p. 57. Am. Chem. Soc., Washington, DC, 1985.
48. Machiels, C. J., Chowdhry, U., Harrison, W. T. A., and Sleight, A. W., in "Solid State Chemistry in Catalysis" (J. F. Brazdil, R. K. Grasselli, Eds.), ACS Symposium Series 279, p. 103. Am. Chem. Soc., Washington, DC, 1985.